Effects of Temperature and Particle Size on the Thermal Property Measurements of Al_2O_3−Water Nanofluids

D. Kwek, A. Crivoi, and Fei Duan*

Division of Thermal and Fluids Engineering, School of Mechanical and Aerospace Engineering, Nanyang Technological University, Singapore 639798

An experimental investigation was conducted on the effective thermal conductivity and viscosity of Al_2O_3 water-based nanofluids. The thermal conductivity was determined using the transient hot wire (THW) method. The results show that the thermal conductivity of Al_2O_3 nanofluids increases with increasing nanoparticle concentrations in a distinct linear trend. Adding (1 to 5) % of Al_2O_3 nanoparticles to water increases the effective thermal conductivity of Al_2O_3 nanofluids by (6 to 20) % at room temperature. There is a substantial increase in the enhancement of thermal conductivity as temperature increases. At 55 °C, this value increases to around 16 %. The thermal conductivity enhancement decreases from (30 to 10) % while the particle size increases from (10 to 35) nm, but enhancement increases when the particle size is above 35 nm. The increase in thermal conductivity is 27.5 % for a particle size of 150 nm. In the viscosity measurements, the effective viscosity increases up to 60 % as the volume concentration increases from 1 % to 5 % at 25 °C. As the temperature increases, the viscosity of Al_2O_3 nanofluids decreases exponentially. Experimental results also indicate that the viscosity of nanofluids is much higher when the nanoparticle size is smaller.

Introduction

Nanofluids are a new class of advanced heat transfer liquids consisting of solid nanoparticles, with sizes typically in the order of (1 to 100) nm. For the past decade, nanofluids have drawn much attention to researchers due to their highly enhanced thermal properties. For example, dispersing a volume fraction of less than 1 % of copper nanoparticles or carbon nanotubes in ethylene glycol or oil has been reported to increase the thermal conductivity by 40 % and 160 %, respectively.[1,2] Furthermore, nanofluids are expected to exhibit better properties compared to conventional heat transfer liquids and fluids that control microsized metallic particles. Nanoparticles which have a much larger surface area than microsized particles possess the potential to further improve heat transfer capabilities[3] and increase the stability of suspensions. Successful implementation of nanofluids can bring benefits and applications to numerous important fields such as microelectronics, transportation, and manufacturing. On the other hand, the viscosity of nanofluids is believed to be lower than those of conventional micrometer-sized particle-liquid suspensions, therefore reducing the pressure drop in the flow channel and pumping power, which in turn lowers operating cost. However, presently, few studies have addressed the viscous properties of nanoparticle suspensions, and data collected have shown that no theoretical models[4−9] are able to predict the viscosity of nanofluids accurately. This can be supported by the experimental results from Masoumi et al.[10] and Nguyuen et al.[11] as their data shows a maximum viscosity increment of 90 % and 45 % for a 5 % nanoparticle volume concentration, whereas theoretical models such as the Einstein, Brinkman, and Batchelor models predict that the viscosity increment is around 15 %. More thorough investigations should be carried out on the effective viscosity of nanofluids. A good understanding of the rheological properties and flow behavior of nanofluids is necessary before they can be commercialized in real heat transfer applications. Thus, a complete understanding of nanofluid properties is essential so that we can optimize the usage of nanofluids and understand their limitations. In this paper, thermal conductivity and dynamic viscosity are measured in Al_2O_3−water nanofluids.

* Corresponding author. E-mail: feiduan@ntu.edu.sg.

Experimental Measurements

Nanofluid Preparation. In our experiments, we dispersed Al_2O_3 nanoparticles with an average diameter of 25 nm and a particle density of 3.7 $g \cdot cm^{-3}$ (Nanostructured and Amorphous Materials, Inc.) into 100 mL of deionized water to prepare the nanofluids with volume concentrations, $(m/\rho)/(100 + m/\rho)$ at 1 %, 2 %, 3 %, 4 %, and 5 %. Oxide-particle volume concentrations are normally below 5 % to maintain moderate viscosity increases. Also, to investigate the particle size effect on the thermal conductivity and viscosity, an additional four sets of nanofluids each with a constant volume concentration of 5 % but with different particle sizes (10 nm, 35 nm, 80 nm, and 150 nm) were prepared. Sample preparation is carried out using a sensitive mass balance with an accuracy of 0.1 mg. To keep the particles well-dispersed in the base fluid, the surfactant cetyltrimethylammonium bromide (CTAB) is added in the nanofluids. As a cationic dispersant, it can keep particles well-dispersed in base fluids.[12,13] The nanofluids were then stirred by a magnetic stirrer before undergoing an ultrasonification process (Fisher Scientific model 500). This is to ensure uniform dispersion of the nanoparticles and also to prevent the nanoparticles from agglomerating in the base fluid.

Measures of Thermal Conductivity and Dynamic Viscosity of the Nanofluids. Numerous experimental work has been reported on thermal conductivity measurements of nanofluids using the transient hot wire (THW) method,[14] the steady-state parallel-plate technique,[15] and the temperature oscillation technique.[16] Among them, the THW method has been used most

10.1021/je1006407
Published on Web 11/29/2010

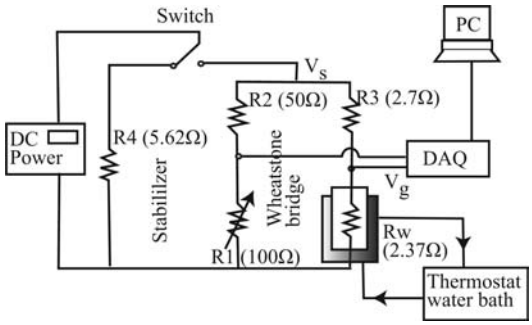

Figure 1. Schematic of THW experimental setup.[14]

extensively since it is accurate and fast at determining the thermal conductivity of a fluid. The significant advantage of this method lies in its almost complete elimination of the effects of natural convection. A schematic of the THW apparatus used in this study is illustrated in Figure 1. A thermostat water circulator was applied to maintain different temperatures for the nanofluid measurements. The measuring principle of the THW technique is based on the transient temperature field around a hot wire. The wire functions as the probe which is used as a line heat source as well as a thermometer. A constant current is supplied to the wire to raise its temperature. The heat dissipated in the wire increases the temperature of the wire as well as that of the nanofluids. This temperature rise depends on the thermal conductivity of the nanofluid sample in which the hot wire is inserted. Therefore, by modeling the temperature change with the voltage change as introduced in the Appendix, the thermal conductivity value of the fluids can be determined.

The experimental apparatus was calibrated by measuring the effective thermal conductivity of deionized water. On the basiss of the calibration results from the THW method for the base fluid, the measurement error was estimated to be within ± 1 %. All measurements were performed at atmospheric pressure. After calibration, the nanofluids were taken into the hot wire cell to measure the thermal conductivity as shown in Figure 1. First, the DC power supply was switched on, and the input voltage V_s was adjusted to 0.5 V, while the switch in the circuit remained on the stabilizer resistor (R_4) circuit. Thereafter, the switch was turned to the Wheatstone bridge circuit, and V_g (as indicated in Figure 1) was balanced by adjusting manually the variable resistor in circuit. Once there was no voltage change, that is, V_g across the Wheatstone bridge was near to 0, the circuit was considered as balanced. Again, after switching back to the stabilizer resistor circuit, the input voltage V_s was then set to the desired value of 2.0 V. Lastly, switched back to the Wheatstone bridge circuit, a voltage change would appear in the hot wire, which caused the circuit to be unbalanced. This unbalanced voltage (V_g) was recorded for 10 s in the computer by the MX 100 data acquisition unit. The input voltage to the circuit was also recorded for each run. This measured unbalanced voltage over natural logarithm of time was plotted. The slope of the fitted curve was equal to the slope of the integrated mathematical linear equation of the THW method in the Appendix, and therefore the thermal conductivity could be determined from other known parameters.

The effective viscosity of Al_2O_3 water-based nanofluids was measured by a standard controlled rate rheometer (Contraves LS 40) which has a cup and bob geometry. The geometry requires only a sample volume of around 5 mL, and hence temperature equilibrium can be achieved quickly within 5 min. The experimental apparatus was calibrated by measuring the viscosity of deionized water. On the basis of the calibration

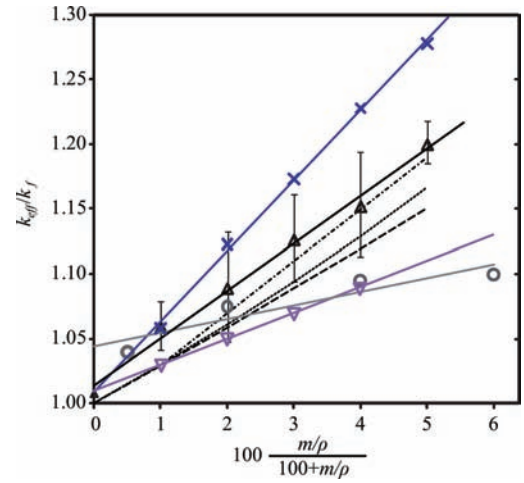

Figure 2. Thermal conductivity enhancement as a function of volume concentrations at 25 °C. Model from: Maxwell (dashed line);[19] Bruggeman (dotted line);[20] Yu and Choi (dashed−dotted line).[21] Data from: △, this study; ×, Eastman et al.;[1] ▽, Das et al.;[16] ○, Li and Peterson.[17]

results, the measurement error was estimated to be within ± 1 %. All measurements were performed at atmospheric pressure. Relative viscosity is calculated with a comparison to pure water.

Results and Discussion

Thermal Conductivity of the Al_2O_3−Water Nanofluids. As presented in Figure 2, the nanofluid thermal conductivity ratio, k_{eff}/k_f, is plotted as a function of nanoparticle volume fraction for a series of Al_2O_3 nanofluids prepared from 25 nm particles and measured at 25 °C. In the ratio, k_{eff} is the measured thermal conductivity of the nanofluids, while k_f is the thermal conductivity of water. Overall, it can be noted that the previous experimental values and the predicted thermal conductivity do increase with a increase of nanoparticle concentration in the fluids and in a distinct linear trend.[1,16,17] Our experimental results have the same trend. It is found that adding a small volume percentage [(1 to 5) %] of Al_2O_3 nanoparticles in water increases the effective thermal conductivity of Al_2O_3 nanofluids by (6 to 20) %. If we disregard the minor differences in the particles size, Figure 2 also clearly shows that there are discrepancies between past experimental data and our data on the amount of enhancement. This difference may be caused by various factors such as different particle preparation, or particle sources. Presently, there are no standard guidelines on the preparation of nanofluids such as the amount and type of surfactant added, the time duration for ultrasonification processes, the measurement methods and procedures, and the size and shape of nanoparticles. Some of these reasons may add up to account for the difference in experimental data. Recently, in a benchmark study of nanofluids,[18] it is found that the thermal conductivity enhancement was consistent between measurement techniques so long as the same measurement technique at the same temperature conditions was employed to measure the thermal conductivity of the base fluid. Therefore, it is indicated that different experimental techniques do not have a significant effect on the thermal conductivity measurement.

However, conventional models[19−21] underestimate the thermal conductivity enhancement when compared against our measured values and the previous experimental data by Eastman et al.[1] The possible reason might be that the present proposed models take into account additional assumptions, such as the interfacial layer, the effects of Brownian motion, the size and shape of nanoparticles, and the effect of clustering of particles.

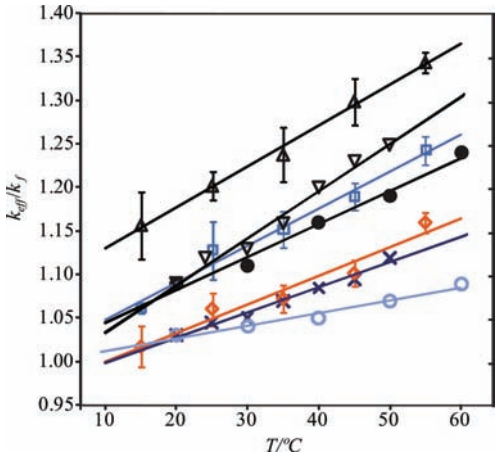

Figure 3. Temperature dependence of thermal conductivity enhancement for Al_2O_3 nanofluids. Data from: △, this study [5 % (by volume)]; ▽, Das et al. [4 % (by volume)];[16] □, this study [3 % (by volume)]; ●, Chon et al. [4 % (by volume)];[22] ◇, this study [1 % (by volume)]; ×, Das et al. [1 % (by volume)];[16] ○, Chon et al. [1 % (by volume)].[22]

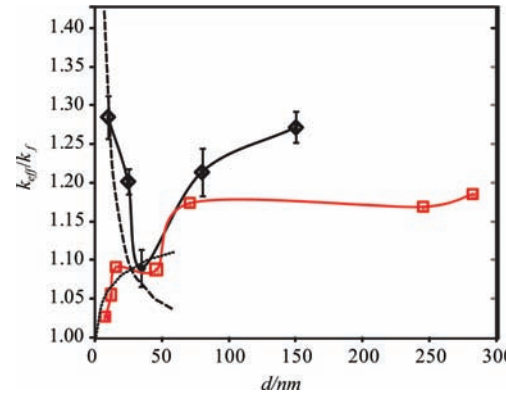

Figure 4. Effects of diameter of nanoparticles on the effective thermal conductivity of nanofluids at 25 °C. Model from: Jang and Choi model (dashed line); modified Maxwell model (dotted line). Data from: ◇, this study [5 % (by volume)]; □, Beck et al. [4 % (by volume)].[26]

The model of Yu and Choi shows a better estimate by modifying the Maxwell equation by including the interfacial resistance between nanoparticles and base fluids.[18] At this point of time, most of these aforementioned mechanisms are neither well-established nor well-understood especially when there are large discrepancies in the past data collected. Therefore, more coherent experimental work is required before concrete conclusions can be inferred from the thermal conduction behavior of nanofluids.

The effective thermal conductivity ratio, k_{eff}/k_f, is expressed at different temperatures, as shown in Figure 3. For the volume concentrations at 1 %, 3 %, and 5 %, there is a substantial increase in the enhancement from (15 to 55) °C. With 1 % particles at about 15 °C, the enhancement is around 1.7 %, but this value increases tremendously to 16 % at 55 °C. Therefore, the presented results imply that the enhancement achieved by having a small volume of nanoparticles in the fluid is considerably higher at higher temperatures. The measurement in 1 %, 3 %, and 5 % nanofluids has a gradient of 0.003575, 0.0045, and 0.00475, respectively. Thus, it can be said that the enhancement of thermal conductivity shows an increase with temperature and the rate of this increase depends on the concentration of nanoparticles. To further substantiate the above trends explained by our experimental results, temperature-dependent results from authors such as Das et al.[16] and Chon et al.[22] were also plotted in Figure 3, although there are differences in the particle size.

The experimental data were compared with the predictions from the thermal conductivity model by Jang and Choi,[23] and good agreement was found for 10 nm, 25 nm, and 35 nm Al_2O_3−water nanofluids as shown in Figure 4. The present experimental data show that the effective thermal conductivity decreases tremendously from (10 to 35) nm. However, as the particle size increases, it deviates from the Jang and Choi model, which was based on the few available data by Lee et al.[24] and Masuda et al.[25] The model of Jang and Choi shows the nanoparticle size dependency of the nanofluid conductivity. As the nanoparticle diameter is reduced, the effective thermal conductivity of nanofluids becomes larger. They explained that this phenomenon was based on Brownian motion; the smaller the average size of nanoparticles in the fluid, the higher the velocity of Brownian motion in nanosized particles. Thus, the heat transferred by convection is enhanced. As a result, the effective thermal conductivity of nanofluids becomes larger. However, as the particles approach micrometer size, they do not remain suspended in the base fluid. Thus, large microparticles do not have significant Brownian motion any more, and there is no enhancement on the effective thermal conductivity by convection. The experimental results of the Al_2O_3−water nanofluids at (80 and 150) nm did not show a similar trend on the decrease in thermal conductivity enhancement when particle size increases. Instead, the data show that the thermal conductivity enhancement in the Al_2O_3 nanofluids increases as the particle size increases above 35 nm, similar to the data of Beck et al.[26] after 50 nm. As the particles become larger, the modified Maxwell model is better to explain the nanoparticle size effects on thermal conductivity given by the Chen correlation,[27] who investigated thermal conductivity of a single particle smaller than the mean free path, and the predicted effective thermal conductivity can be expressed as,

$$k_p = k_{bulk}\frac{0.75(d_p/l_p)}{0.75(d_p/l_p) + 1} \quad (1)$$

where k_p, d_p, l_p, and k_{bulk} are the thermal conductivities, characteristic length of the nanoparticles, mean free path of the nanoparticles, and thermal conductivity of the bulk material, respectively. Because the thermal conductivity of a nanoparticle proposed by Chen et al. is much less than its bulk value, the modified Maxwell model therefore predicts a decreasing nanofluid thermal conductivity with a decrease of particle size. Thus, a threshold in particle size might exist where either the Brownian motion or the diffusive heat transport would be more dominant on the thermal conductivity in the nanofluids.

Dynamic Viscosity of the Al_2O_3−Water Nanofluids. Figure 5 shows that the dynamic viscosity ratio increases as the volume concentration increases at room temperature. The results of Masoumi et al. (28 nm)[10] and Nguyen et al. (36 nm)[11] show similar trends. From the present experimental results, the measured viscosity of Al_2O_3 nanofluids is significantly higher than the base fluid by about (20 and 61) % at a (1 and 5) % volume fraction, respectively. The Masoumi et al. and Nguyen et al. data and our measured data are much higher than those of predicted values using the Einstein, Brinkman, Batchelor, and Graham equations.[4,5,8,9] Einstein's formula and the others originating from it can be used to better explain liquids that contain a small number of dispersed particles (< 1 %). However, for higher particle concentrations the deviation of conventional models from our experimental data is considerably larger. Even Batchelor's formula, the one taking Brownian effects into

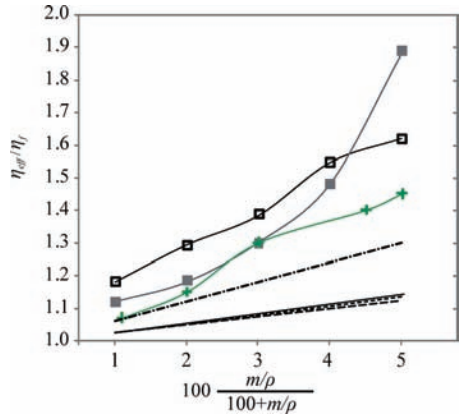

Figure 5. Relative viscosity of Al_2O_3 nanofluid as a function of volume concentration at 25 °C. Data from: □, this study; ■, Masoumi et al.;[10] +, Nguyen et al.[11] Model from: Graham (dashed−dotted line);[9] Brinkman (dotted line);[5] Batchelor (solid line);[8] Einstein (dashed line).[4]

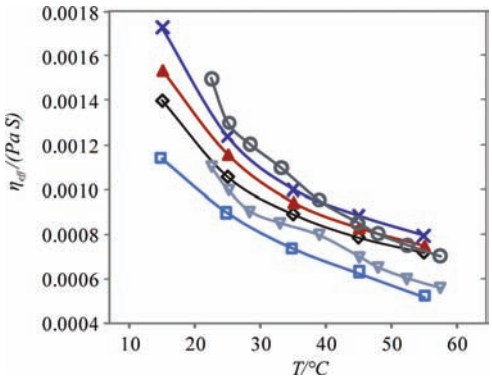

Figure 6. Dynamic viscosity as a function of the liquid temperature for Al_2O_3−water nanofluids. Data from: □, this study, water; ◇, this study [1 % (by volume)]; ▲, this study [2 % (by volume)]; ×, this study [3 % (by volume)]; ▽, Nguyen et al. [1 % (by volume)];[11] ○, Nguyen et al. [4.5 % (by volume)].[11]

account, performs poorly. Chandrasekar et al.[28] suggested that a huge difference between experimental results and predicted values may be because conventional models neglected the hydrodynamic interactions between particles which become important as the disturbance of the fluid around one particle interacts with that around other particles at higher volume concentrations. Hence, the conventional models cannot explain the high viscosity ratio.

The dynamic viscosities were illustrated for the three nanofluids with a particle volume fraction ranging from (1 to 3) % for temperatures varying from (15 to 55) °C in Figure 6. It is observed that the nanofluid dynamic viscosity decreases with increasing temperature. Nguyen et al. suggested that the temperature effect is probably due to weakening of interparticle forces.[11] Also shown in Figure 6, the gradient of the dynamic viscosity with temperature becomes steeper in the temperatures from (15 to 30) °C. This observation can be supported by the results of Nguyen et al.[11]

In Figure 7, the experimental results show that the effective viscosity decreases significantly as particle sizes increase and reaches an almost constant value. This trend is very similar to the other studies presented[10,29,30] in Figure 7 except for the particle size greater than 100 nm. Timofeeva et al. identified that nanofluids with smaller particles have a higher relative viscosity because of their tendency to form larger agglomerates while the larger diameter particles form smaller agglomerates.[31] The possible reasons for a stronger agglomeration in smaller

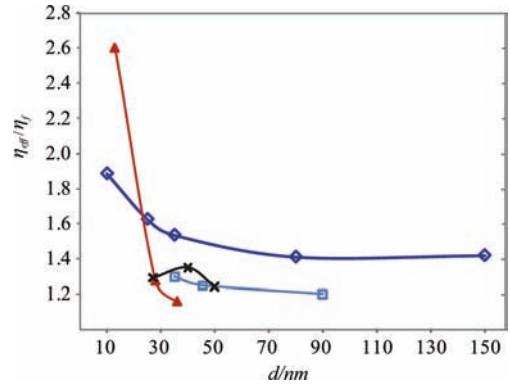

Figure 7. Relative dynamic viscosity as a function of diameter of Al_2O_3 particles in the nanofluids at 25 °C. Data from: ◇, this study [5 % (by volume)]; □, Lu and Fan [5 % (by volume)];[29] ▲, Masoumi et al. [2.85 % (by volume)];[10] ×, Prasher et al. [3 % (by volume)].[30]

Al_2O_3 particles may be their better ability to undergo the dissolution−precipitation growth or their weaker repulsion due to a smaller surface charge.

As mentioned by Chen et al.,[32] nanoparticles in nanofluids are mostly in the form of aggregates. Therefore the Krieger model,[33] $(\eta_{nf}/\eta_f) = (1 - (\phi_a/\phi_m))^{-2.5\phi_m}$, is more appropriate to calculate the relative viscosity between a nanofluid (nf) and its base fluid (f), where 2.5 is the intrinsic viscosity, η_0, of spherical particles, ϕ_a is the volume fraction of aggregates, ϕ_m is the volume fraction of densely packed spheres and the volume fraction of the aggregates is expressed as $\phi_a = \phi(d_a/d)^{3-d_f}$, in which d_f is the fractal dimension of the aggregates. For well-dispersed individual particles, ϕ_a is equal to ϕ, and the Krieger model reduces to the Einstein model. This is a very ideal case where there is zero agglomeration. However, none of the research is able to obey fully the Einstein equation until now. The reason may be that it is unlikely to eliminate the agglomeration completely. Zhao et al. measured the diameter of silicon dioxide aggregates using a Malvern-Zetasizer Nano S90.[34] When the nanoparticle size increases, the magnitude of (d_a/d) decreases. Thus the volume fraction of the aggregates decreases, and the relative viscosity ratio decreases based on the Krieger model.[33] In addition, Zhao et al. mentioned that the shape of the aggregates is no longer spherical because of aggregation and the intrinsic viscosity, whereas η_0 which consequently changes with the shape must be considered. From theoretical considerations, Einstein obtained that $\eta_0 = 2.5$ for spherical particles and η_0 is greater than 2.5 for other shapes.[35] As d decreases, the aggregated shape becomes disordered and varied. Thus, η_0 should be larger than that of the spherical particles. This can also account for the increase in viscosity ratio as the particle diameter decreases.

Slight agglomeration is likely to remain in the nanofluids in this study since measures are made for different particle sizes at a constant 5 % volume concentration, which is considered high. On the basis of the Krieger model, it is possible that the relative viscosity is higher for particles at a smaller size, as we observed in this study.

Conclusions

The effective thermal conductivity and viscosity of nanofluids were found experimentally to increase significantly with the particle volume fraction (Figures 2 and 5). A linear increase in the effective thermal conductivity of nanofluids with temperature was also observed (Figure 3). Besides the volume fraction of particles and temperature, it can be concluded that the particle

size also influences the thermal conductivity of nanofluids (Figure 4). It is indicated that existing classical models cannot explain the observed enhanced thermal conductivity of nanofluids. More comprehensive models therefore need to be developed. Particle sizes, particle dispersions, clustering, and temperature should be taken into account in the model development for nanofluids. Similarly, the conventional models are unable to predict the anomalous increase in dynamic viscosity. At volume concentrations of 5 %, the dynamic viscosity has an increment of 60 % (Figure 5). The significant deviation between the experimental results and the existing theoretical models is still unaccounted for. The dynamic viscosity of the Al_2O_3 nanofluid decreasing exponentially as temperature increases (Figure 6), together with the increased thermal conductivity, makes it more attractive as a cooling fluid for devices. The effects of particle size on the dynamic viscosity is limited as shown in Figure 7. More complete experiments involving a wide range of nanoparticle sizes can be conducted in future work, especially at smaller nanoparticle sizes.

Appendix: Mathematical Formulation

The detailed derivation of the THW method is reported in ref 36. The governing equation for radial transient heat conduction in a homogeneous infinite cylindrical medium is given by

$$\frac{\partial}{\partial r}\left(r\frac{\partial \theta}{\partial r}\right) = \frac{r}{\alpha}\frac{\partial \theta}{\partial t} \tag{2}$$

where $\theta = T - T_0$ is the temperature rise in the medium and T_0 is the initial temperature, T is the temperature in the surrounding medium at time t and radial position r, and $\alpha = (k/\rho c_p)$ is the thermal diffusivity of the surrounding medium.

The outer boundary ($r \rightarrow \infty$) condition is

$$\theta(r, t) = 0 \tag{3}$$

The inner boundary condition at $r = a$ is

$$q = -2\pi a k\left(\frac{\partial \theta}{\partial r}\right)_{r=a},\ t > 0 \tag{4}$$

where q is the heat rate per unit length. Thus, the solution of eq 2 can be given by

$$\theta(a, t) = \frac{q}{4\pi k}\ln\left(\frac{4\alpha}{a^2 C}t\right) \tag{5}$$

where $C = \exp(\gamma)$ and $\gamma = 0.5772$ is Euler's constant. From eq 5, the thermal conductivity of nanofluids can be calculated using the linear relationship between the temperature rise and the natural logarithm of time.

From the analogy of the Wheatstone bridge circuit used in the hot-wire apparatus and imposing the mathematical formulation for temperature rise of the hot wire (eq 5), an integrated mathematical formulation is established for measuring the thermal conductivity and thermal diffusivity simultaneously and more conveniently.

Applying Kirchoff's voltage law to the balanced Wheatstone bridge circuit (Figure 1) and using the temperature resistance relationship of wire, the voltage change is given by

$$V_g = \left(\frac{R_3}{(R_3 + R_w)^2}\right)(\beta R_w)V_s\theta \tag{6}$$

where V_s is the input voltage across the Wheatstone bridge, and β is the resistance-temperature coefficient of Pt wire.

Substituting eq 5 into eq 6, we have

$$V_g = \left(\frac{R_3}{(R_3 + R_w)^2}\right)(\beta R_w)\frac{V_s q}{4\pi k}\left(\ln t + \ln\frac{4\alpha}{a^2 C}\right) \tag{7}$$

For

$$A = \left(\frac{\beta R_w R_3 V_s}{(R_3 + R_w)^2}\right)\frac{q}{4\pi k}$$

$$B = A\ln\frac{4a}{a^2 C}$$

Equation 7 can be written as the simplest form of

$$V_g = A\ln t + B \tag{8}$$

Since V_g can be obtained directly from the Wheatstone bridge circuit through the digital voltmeter, the thermal conductivity and thermal diffusivity can be calculated more conveniently from slope (A) and intersect (B) by eq 8.

Acknowledgment

The authors would like to thank Profs. Kai Choong Leong and Charles Yang for their generosity in sharing their HWT equipment. The authors would also like thank to Dr. Liwen Jin for sharing his knowledge on the thermal conductivity measurements.

Literature Cited

(1) Eastman, J. A.; Choi, S. U. S.; Li, S.; Yu, W.; Thompson, L. J. Anomalously increased effective thermal conductivities of ethylene glycol-based nanofluids containing copper nanoparticles. *Appl. Phys. Lett.* **2001**, *78*, 718–720.
(2) Choi, S. U. S.; Zhang, Z. G.; Yu, W.; Lockwood, F. E.; Grulke, E. A. Anomalous thermal conductivity enhancement in nano tube suspensions. *Appl. Phys. Lett.* **2001**, *78*, 2252–2254.
(3) Xie, H.; Fujii, M.; Zhang, X. Effect of interfacial nanolayer on the effective thermal conductivity of nanoparticle-fluid mixture. *Int. J. Heat Mass Transfer* **2005**, *48*, 2926–2932.
(4) Einstein, A. A new determination of the molecular dimensions. *Ann. Phys.* **1906**, *19*, 289–306.
(5) Brinkman, H. C. The viscosity of concentrated suspensions and solution. *J. Chem. Phys.* **1952**, *20*, 571.
(6) Frankel, N. A.; Acrivos, A. On the viscosity of a concentrated suspension of solid spheres. *Chem. Eng. Sci.* **1967**, *22*, 847–853.
(7) Lundgren, T. S. Slow flow through stationary random beds and suspensions of spheres. *J. Fluid Mech.* **1972**, *51*, 273–299.
(8) Batchelor, G. K. The effect of Brownian motion on the bulk stress in a suspension of spherical particles. *J. Fluid Mech.* **1977**, *83*, 97–117.
(9) Graham, A. L. On the viscosity of suspension of solid spheres. *Appl. Sci. Res.* **1981**, *37*, 275–286.
(10) Masoumi, N.; Sohrabi, N.; Behzadmehr, A. A new model for calculating the effective viscosity of nanofluids. *J. Phys. D: Appl. Phys.* **2009**, *42*, 055501.
(11) Nguyen, C. T.; Desgranges, F.; Roy, G.; Galanis, N.; Mare, T.; Boucher, S.; Angue Mintsa, H. Temperature and particle-size dependent viscosity data for water-based nanofluids - Hysteresis phenomenon. *Int. J. Heat Fluid Flow* **2007**, *28*, 1492–1506.
(12) Li, X.; Zhu, D.; Wang, X. Evaluation on dispersion behaviour of the aqueous copper nano-suspensions. *J. Colloid Interface Sci.* **2007**, *310*, 456–463.

(13) Sakamoto, M.; Kanda, Y.; Miyahara, M.; Higashitani, K. Origin of long-range attractive force between surfaces hydrophobized by surfactant adsorption. *Langmuir* **2002**, *18*, 5713–5719.

(14) Kestin, J.; Wakeham, W. A. A contribution to the theory of the transient hot-wire technique for thermal conductivity measurements. *Physica A* **1978**, *92*, 102–116.

(15) Wang, X.; Xu, X.; Choi, S. U. S. Thermal conductivity of nanoparticle - fluid mixture. *J. Thermophys. Heat Transfer* **1999**, *13*, 474–480.

(16) Das, S. K.; Putta, N.; Thiesen, P.; Roetzel, W. Temperature dependence of thermal conductivity enhancement for nanofluids. *J. Heat Transfer* **2003**, *125*, 567–574.

(17) Li, C. H.; Peterson, G. P. Experimental investigation of temperature and volume fraction variations on the effective thermal conductivity of nanoparticle suspensions (nanofluids). *J. Appl. Phys.* **2006**, *99*, 1–8.

(18) Buongiorno, J.; Venerus, D. C.; Prabhat, N.; McKrell, T.; Townsend, J.; Christianson, R.; Tolmachev, Y. V.; Keblinski, P.; Hu, L.; Alvarado, J. L.; Bang, I. C.; Bishnoi, S. W.; Bonetti, M.; Botz, F.; Cecere, A.; Chang, Y.; Chen, G.; Chen, H.; Chung, S. J.; Chyu, M. K.; Das, S. K.; Paola, R. D.; Ding, Y.; Dubois, F.; Dzido, G.; Eapen, J.; Escher, W.; Funfschilling, D.; Galand, Q.; Gao, J.; Gharagozloo, P. E.; Goodson, K. E.; Gutierrez, J. G.; Hong, H.; Horton, M.; Hwang, K. S.; Iorio, C. S.; Jang, S. P.; Jarzebski, A. B.; Jiang, Y.; Jin, L.; Kabelac, S.; Kamath, A.; Kedzierski, M. A.; Kieng, L. G.; Kim, C.; Kim, J. H.; Kim, S.; Lee, S. H.; Leong, K. C.; Manna, I.; Michel, B.; Ni, R.; Patel, H. E.; Philip, J.; Poulikakos, D.; Reynaud, C.; Savino, R.; Singh, P. K.; Song, P.; Sundararajan, T.; Timofeeva, E.; Tritcak, T.; Turanov, A. N.; Van Vaerenbergh, S.; Wen, D.; Witharana, S.; Yang, C.; Yeh, W. H.; Zhao, X. Z.; Zhou, S. Q. A benchmark study on the thermal conductivity of nanofluid. *J. Appl. Phys.* **2009**, *106*, 094312.

(19) Maxwell, J. C. *A Treatise on Electricity and Magnetism*, 3rd ed.; Oxford University Press: London, 1892.

(20) Bruggeman, D. A. G. Calculation of various physics constants in heterogenous substances. I. Dielectricity constants and conductivity of mixed bodies from isotropic substances. *Ann. Phys.* **1935**, *24*, 636–664.

(21) Yu, W.; Choi, S. U. S. The role of interfacial layers in the enhanced thermal conductivity of nanofluids: a renovated Maxwell model. *J. Nanopart. Res.* **2003**, *5*, 167–171.

(22) Chon, C. H.; Kihm, K. D.; Lee, S. P.; Choi, S. U. S. Empirical correlation finding the role of temperature and particle size for nanofluid (Al_2O_3) thermal conductivity enhancement. *Appl. Phys. Lett.* **2005**, *87*, 1–3.

(23) Jang, S. P.; Choi, S. U. S. Role of Brownian motion in the enhanced thermal conductivity of nanofluids. *Appl. Phys. Lett.* **2004**, *84*, 4316–4318.

(24) Lee, S.; Choi, S. U. S.; Li, S.; Eastman, J. A. Measuring thermal conductivity of fluids containing oxide nanoparticles. *J. Heat Transfer* **1999**, *121*, 280–289.

(25) Masuda, H.; Ebata, A.; Teramae, K.; Hishinuma, N. Alternation of thermal conductivity and viscosity of liquid by dispersing ultra-fine particles. *Netsu Bussei* **1993**, *4*, 227–233.

(26) Beck, M. P.; Yuan, Y.; Warrier, P.; Teja, A. S. The effect of particle size on the thermal conductivity of alumina nanofluids. *J. Nanopart. Res.* **2009**, *11*, 1129–1136.

(27) Chen, G. Nonlocal and nonequilibrium heat conduction in the vicinity of nanoparticles. *ASME J. Heat Transfer* **1996**, *118*, 539–545.

(28) Chandrasekar, M.; Suresh, S.; Chandra Bose, A. Experimental investigations and theoretical determination of thermal conductivity and viscosity of Al_2O_3/water nanofluid. *Exp. Therm. Fluid Sci.* **2010**, *34*, 210–216.

(29) Lu, W. Q.; Fan, Q. M. Study for the particle's scale effect on some thermophysical properties of nanofluids by a simplified molecular dynamics method. *Eng. Anal. Boundary Elem.* **2008**, *32*, 282–289.

(30) Prasher, R.; Bhattacharya, P.; Phelan, P. E. Thermal conductivity of nanoscale colloidal solutions (nanofluids). *Phys. Rev. Lett.* **2005**, *94*, 025901.

(31) Timofeeva, E. V.; Gavrilov, A. N.; McCloskey, J. M.; Tolmachev, Y. V. Thermal conductivity and particle agglomeration in alumina nanofluids: experiment and theory. *Phys. Rev. E* **2007**, *76*, 061203.

(32) Chen, H.; Ding, Y.; He, Y.; Tan, C. Rheological behaviour of ethylene glycol based titania nanofluids. *Chem. Phys. Lett.* **2007**, *444*, 333–337.

(33) Krieger, I. M.; Dougherty, T. J. A mechanism for non-newtonian flow in suspensions of rigid spheres. *J. Rheol.* **1959**, *3*, 137–152.

(34) Zhao, J. F.; Zhong, Y. L.; Ni, M. J.; Cen, K. F. Dependence of Nanofluid Viscosity on Particle Size and pH Value. *Chin. Phys. Lett.* **2009**, *26*, 066202.

(35) Rubio-Hernandez, F. J.; Ayucar-Rubio, M. F.; Velazquez-Navarro, J. F.; Galindo-Rosales, F. J. Intrinsic viscosity of SiO_2, Al_2O_3 and TiO_2 aqueous suspensions. *J. Colloid Interface Sci.* **2006**, *298*, 967–972.

(36) Murshed, S. M. S.; Leong, K. C.; Yang, C. Enhanced thermal conductivity of TiO_2−water based nanofluids. *Int. J. Therm. Sci.* **2005**, *44*, 367–373.

Received for review June 10, 2010. Accepted October 30, 2010. The study is supported from NTU-SUG funding.

JE1006407